crystals

MDPI

Article

Extending the pool of compatible peptide hydrogels for protein crystallization

Guillermo Escolano-Casado [1], Rafael Contreras-Montoya [2], Mayte Conejero-Muriel [1], Albert Castellví [3], Judith Juanhuix [3], Modesto T. Lopez-Lopez [4], Luis Álvarez de Cienfuegos [2,*] and José A. Gavira [1,*]

1 Laboratorio de Estudios Cristalográficos, Instituto Andaluz de Ciencias de la Tierra (Consejo Superior de Investigaciones Científicas-Universidad de Granada), Avenida de las Palmeras 4, 18100 Armilla, Granada, Spain; guillermoescolanocasado@gmail.com (G.E.-C.); mmayytte@gmail.com (M.C.-M.)
2 Departamento de Química Orgánica, Universidad de Granada, C. U. Fuentenueva, Avda. Severo Ochoa s/n, E-18071 Granada, Spain; rcm@ugr.es
3 ALBA Synchrotron, Carrer de la Llum 2-26, Cerdanyola del Vallès, 08290 Barcelona, Spain; acastellvi@cells.es (A.C.); juanhuix@cells.es (J.J.)
4 Departamento de Física Aplicada, Facultad de Ciencias, (UGR), Spain; modesto@ugr.es
* Correspondence: lac@ugr.es (L.Á.d.-C.); jgavira@iact.ugr-csic.es (J.A.G.)

Received: 5 April 2019; Accepted: 7 May 2019; Published: 10 May 2019

Abstract: Short-peptide supramolecular (SPS) hydrogels are a class of materials that have been found to be useful for (bio)technological applications thanks to their biocompatible nature. Among the advantages reported for these peptides, their economic affordability and easy functionalization or modulation have turned them into excellent candidates for the development of functional biomaterials. We have recently demonstrated that SPS hydrogels can be used to produce high-quality protein crystals, improve their properties, or incorporate relevant materials within the crystals. In this work, we prove that hydrogels based on methionine and tyrosine are also good candidates for growing high-quality crystals of the three model proteins: lysozyme, glucose isomerase, and thaumatin.

Keywords: protein crystallization; composite crystals; peptide hydrogels

1. Introduction

In the biological macromolecules field, where sample impurity has been a relevant issue for many years, it is generally thought that the participation of any new additive, such as gel precursors, could be detrimental to the crystallization, affecting the final crystal properties. In contrast, it is well accepted that the use of gels may help control and facilitate the growth of bigger and higher-quality crystals for inorganic materials [1–3]. Nowadays, researchers are being convinced about the advantages of using gels in protein crystallization, such as the reduction of sedimentation, the inhibition of twinning formation, and the reduction of convective flow, which simulates microgravity conditions [4]. However, the use of gels is still largely unexplored in applications for protein crystallography [5].

Although fundamental studies on the crystallization of proteins in gel media have never stopped, we reckon that this strategy has not burst yet. Already in 1999, the term reinforced protein crystal was introduced for crystals grown in silica gels, which showed a higher robustness due to the incorporation of the gel fibers into the crystalline network [6]. It was also demonstrated that protein crystals grown in agarose are more stable against osmotic shocks generated when a crystal is transferred from its mother liquid to a solution containing for example a ligand, inhibitor, cryoprotectant agent, or heavy atom [7,8]. Gels facilitate handling crystals [9], avoiding their deterioration, and making it even the collection of diffraction data at room temperature possible [6,10].

Generally, agarose gels [4] are the most used gel for protein crystallization due to their easy preparation and handling. Other gels such as silica, polyethylene oxide (PEO), polyacrylamide, dextran, sephadex, cellulose gels, or their derivatives, including methyl or hydroxymethyl derivatives, have also been tested in biomacromolecules' crystallization [3,4]. More recently, novel gels based on polymers such as polyvinyl alcohol, calcium alginate beads, or new synthetic ones such as poly(N-isopropyl-acrylamide-co-n-butyl methacrylate) [3] and hydrophilic PEG (poly(ethylene glycol)) [11] have also been tested in protein crystallization. PEG-based hydrogels are also very promising for biological and biomedical applications, including biosensors and macromolecular drug delivery, due to their low toxicity and lack of immunogenicity [12,13].

Lately, we have been exploring the incorporation of short peptide supramolecular (SPS) hydrogels to extend the pool of gels to novel biocompatible and biodegradable materials with broad biological and technological applications [14,15]. The use of these easily and broadly functionalizable compounds significantly expands the field of protein crystallization, allowing the study of the influence of the peptide chemical composition and chirality in crystallogenesis [16,17]. Besides, the incorporation of the gel fibers does not influence the three-dimensional (3D) structure, as previously observed with many other hydrogels; eventually, it influences the packing, generating new polymorphs [16]. Moreover, these peptide hydrogels are able to modulate the physicochemical properties of the crystals, altering their stability and dissolution rate. An increased stability and in vivo short half-life of the crystals, as produced by these compounds, is of great advantage to control the drug delivery of therapeutic proteins (biopharmaceuticals). In particular, we have recently shown that insulin crystallized in Fmoc-AA (Fmoc-Ala-Ala-OH) short peptide hydrogels increases its stability, leading to thermally stable insulin crystals [18]. Although insulin crystals described in this patent were obtained in di-alanine hydrogel, the possibility of using other type of dipeptides is also mentioned. At this respect, this is the first report in which Fmoc-MF and Fmoc-Y have been used for protein crystallization.

2. Materials and Methods

All the materials were of analytical grade and used without further purification. Fmoc-MF (Fmoc-Met-Phe-OH) was synthesized by solid phase protocol, as previously described [19]. A TEM image of the xerogel as well as rheological data are included in the Supplementary Materials (Figures S1 and S2). Fmoc-Y (Fmoc-Tyr-OH) was bought from Sigma-Aldrich. The rheological data of this hydrogel is included in the Supplementary Materials (Figure S2).

2.1. Hydrogel Preparation

For the formation of the Fmoc-MF hydrogel, we followed a previously reported protocol [20]. Briefly, the Fmoc-MF hydrogel precursor was weighted in an Eppendorf tube and suspended in ultrapure water to the final concentration. The suspension was sonicated in an HSt Powersonic 603- ultrasonic bath (Hwashin Technology Company, Korea) for 10 min, followed by the addition of NaOH 0.5 M. After each addition, the sample was vortexed and sonicated until a clear solution was obtained, typically at pH 9.5. Then, the solution was diluted with ultrapure water to fit the final concentration. Hydrogelation was driven by adding two molar equivalents of glucono-δ-lactone (GdL) (Alfa Aesar, Karlsruhe, Germany) and vortexed for five seconds. The obtained sol was left sitting for 12 h, approximately, to obtain the column of gel.

Hydrogels Fmoc-Y were prepared in Eppendorf tubes by dissolving the peptide in DMSO (dimethyl sulfoxide) followed by the addition of Milli-Q water to reach a final volume of 100 µL [21]. The volume relationship of DMSO:water depended on the final concentration of the hydrogels being 5:95 for 0.2 wt%, 10:90 for 0.5 wt% and 0.75 wt%, and 15:85 for 1.0 wt%.

Prior to loading the protein, all the hydrogels were purified by dialysis by adding 1 mL of Milli-Q water on top of the hydrogels and changing the water every day for a week.

2.2. Crystallization Experiments

Lysozyme (chicken HEWL) and Thaumatin from *T. daniellii* were purchased as a lyophilized powder from Sigma (L6876 and T7638 respectively), and glucose isomerase (D-xylose-ketol-isomerase) from *S. rubiginosus* was purchased as a crystal suspension from Hampton Research (HR7-100, Aliso Viejo, USA). The lysozyme was dissolved and dialyzed in 50 mM of sodium acetate, pH 4.5. Glucose isomerase (GI) crystals were dissolved in Milli-Q water and extensively dialyzed against 100 mM of Hepes pH 7.0. Thaumatin was dissolved in Milli-Q water. Protein concentration was determined spectrophotometrically at 280 nm prior to setting the crystallization experiments and after filtration through an 0.45-μm pore size membrane.

We used the counter-diffusion technique in two-layer configurations to run the crystallization experiments. In order to charge the hydrogel, the protein solution at twice the final required concentration was poured on top of the gel layer, and left to diffuse into the hydrogel for one week following the previously detailed protocol [17]. Then, the equilibrated protein solution was substituted by the precipitant cocktail, and the experiments were kept at 295 K using incubators.

Fmoc-MF was evaluated with the three model systems: lysozyme, thaumatin, and glucose isomerase, while the commercial Fmoc-Y was tested only with lysozyme. Reference crystals were obtained in agarose using an identical set-up. The experimental conditions are summarized in Table 1.

Table 1. Resume of crystallization conditions.

Hydrogel	(% *w*/*v*)	Protein	Concentration (mg/mL)	Precipitant
Fmoc-MF	0.2, 0.5, 0.75 and 1.0	Lysozyme	80	6.0% (*w*/*v*) NaCl, 50 mM of Na acetate pH 4.5
Fmoc-Y	0.2, 0.5, 0.75 and 1.0			
Agarose	0.5			
Fmoc-MF	0.5 and 0.75	Thaumatin	50	45% (*w*/*v*) KNa tartrate pH 7.6
Agarose	0.5			
Fmoc-MF	0.5 and 0.75	Glucose isomerase	50	10% (*v*/*v*) PEG 1000, 0.2 M of $MgCl_2$, 0.1 M of Hepes pH 7.0
Agarose	0.5			

2.3. X-ray Data Collection and Analysis

Crystal quality was determined by X-ray diffraction data collected at beam lines XALOC (ALBA) [22] and ID23-2 (ESRF) [23] of the Spanish and European synchrotron radiation sources, respectively. Shortly, crystals were extracted from the hydrogel using a Pipetman (200 μL) with the tip-end cut and deposited over a plastic Petri dish. Drops of the recovered precipitant or the precipitant plus cryoprotectant (20% *v*/*v* glycerol) were deposited nearby. Selected crystals were transferred to either the precipitant solution for final cleaning, or directly to the cryoprotectant solution with the help of a LithoLoop (Molecular Dimensions Inc.). Then, crystals were flash cooled in liquid nitrogen and saved for data collection. The data collection configuration was kept constant for each series and protein. We collected data from at least two crystals of each hydrogel concentration and type. Full data processing statistics are included in Tables 2–4, for the best crystals of each protein and hydrogels, complemented with the data in Tables S1–S4 summarizing the data for all the collected crystals.

3. Results

Fmoc-Y hydrogel has already been prepared and characterized [24,25], while Fmoc-MF was produced and characterized in our laboratory [19]. In both cases, they form a gel in the concentration range used in this work, 0.2% to 1.0% (*w*/*v*). Rheological data showing an increase of the viscoelastic moduli as a function of gel concentration is reported in the Supplementary Materials (Figure S2).

Table 2. Summarized the data collection conditions and final statistical values of lysozyme crystals in Fmoc-MF and in agarose hydrogels (data in brackets correspond to high-resolution shell).

	Agarose (% *w/v*)	**Fmoc-MF (% *w/v*)**			
Concentration	**0.5**	**0.2**	0.5	0.75	1.0
Data Acquisition					
ESRF	ID23-2	ID23-2	ID23-2	ID23-2	ID23-2
Detector type	PILATUS	PILATUS	PILATUS	PILATUS	PILATUS
Wavelength (Å)	0.87290	0.87290	0.87290	0.87290	0.87290
Distance (mm)	215.97	215.97	215.97	215.97	215.97
Exposure time (s)	0.04	0.04	0.04	0.04	0.04
Oscillation (°)	0.1	0.1	0.1	0.1	0.1
Data Statistics					
Space group	P 4_3 2_1 2	P 4_3 2_1 2	P 4_3 2_1 2	P 4_3 2_1 2	P 4_3 2_1 2
Unit cell: a = b, c (Å)	79.00, 37.26	77.33, 38.01	77.53, 37.81	77.52, 37.90	77.56, 37.86
Resolution (Å)	39.50–1.20	38.66–1.30	38.77–1.20	38.76–1.15	38.78–1.25
(High-shell)	(1.22–1.20)	(1.32–1.30)	(1.22–1.20)	(1.17–1.15)	(1.27–1.25)
Unique reflections	37471 (1805)	28991 (1425)	36659 (1800)	41636 (2009)	32570 (1586)
R-merge (%)	5.9 (79.8)	10.5 (95.3)	4.7 (87.6)	5.2 (82.6)	5.1 (83.9)
I/σ(I)	20.7 (3.3)	11.1 (1.9)	27.8 (3.2)	23.6 (3.2)	26.7 (3.6)
Completeness (%)	100.0 (100.0)	100.0 (100.0)	100.0 (100.0)	100.0 (100.0)	100.0 (100.0)
Redundancy	13.6 (13.8)	13.9 (14.4)	13.7 (13.8)	13.7 (13.2)	13.7 (12.8)
B-factor ($Å^2$)	9.5	11.5	10.1	8.8	10.6
Mosaicity	0.18	0.19	0.20	0.12	0.21

Table 3. Summarized the data collection conditions and final statistical values of thaumatin and glucose isomerase crystals obtained in Fmoc-MF and in agarose hydrogels (data in brackets correspond to the high-resolution shell).

	Thaumatin			**Glucose Isomerase**		
	Agarose (% *w/v*)	**Fmoc-MF (% *w/v*)**		**Agarose (% *w/v*)**	**Fmoc-MF (% *w/v*)**	
Concentration	0.5	0.5	0.75	0.5	0.5	0.75
Data Acquisition						
ESRF	ID23-2	ID23-2	ID23-2	ID23-2	ID23-2	ID23-2
Detector type	PILATUS	PILATUS	PILATUS	PILATUS	PILATUS	PILATUS
Wavelength (Å)	0.87290	0.87290	0.87290	0.87290	0.87290	0.87290
Distance (mm)	215.97	215.97	215.97	215.97	215.97	215.97
Exposure time (s)	0.04	0.04	0.04	0.04	0.04	0.04
Oscillation (°)	0.1	0.1	0.1	0.1	0.1	0.1
Data Statistics						
Space group	P 4_1 2_1 2	P 4_1 2_1 2	P 4_1 2_1 2	I222	I222	I222
Unit cell: a, b, c (Å)	57.98, 57.98, 150.61	58.17, 58.17, 151.14	58.14, 58.14, 150.63	93.41, 99.29, 103.09	93.18, 98.67, 102.88	93.20, 98.36, 102.91
Resolution (Å)	45.94–1.05	46.10–1.10	46.02–1.15	46.71–1.15	49.33–1.10	46.60–1.05
(High shell)	(1.07–1.05)	(1.12–1.10)	(1.17–1.15)	(1.17–1.15)	(1.12–1.10)	(1.07–1.05)
Unique reflections	120047 (5702)	106068 (5180)	92658 (4534)	167421 (8287)	190602 (9407)	214576 (9993)
R-merge (%)	5.6 (68.7)	6.0 (96.1)	7.2 (90.1)	6.8 (77.1)	6.3 (73.6)	5.4 (83.8)
I/σ(I)	24.6 (3.5)	22.6 (2.8)	19.6 (3.0)	11.9 (1.9)	12.6 (1.9)	15.1 (1.7)
Completeness (%)	99.7 (97.8)	100.0 (100.0)	100.0 (100.0)	99.3 (99.9)	99.9 (100.0)	98.4 (93.4)
Redundancy	13.6 (10.4)	13.9 (13.0)	14.0 (13.3)	5.2 (4.8)	5.1 (4.7)	5.1 (4.4)
B-factor ($Å^2$)	5.6	6.9	7.2	8.2	6.3	6.0
Mosaicity	0.05	0.06	0.06	0.1	0.12	0.09

Table 4. Summarized data collection conditions and final statistical values of lysozyme crystals obtained in Fmoc-Tyr-OH (Fmoc-Y) and in agarose hydrogels (data in brackets correspond to high-resolution shell).

	Agarose (% *w/v*)	**Fmoc-Y (% *w/v*)**			
Concentration	**0.5**	**0.2**	0.5	0.75	1.0
Data Acquisition					
ALBA	XALOC	XALOC	XALOC	XALOC	XALOC
Detector type	PILATUS 6M	PILATUS 6M	PILATUS 6M	PILATUS 6M	PILATUS 6M
Wavelength (Å)	0.980	0.979154	0.979154	0.979154	0.979154
Distance (mm)	160.35	128.0	128.0	128.0	128.0
Exposure time (s)	0.2seg	0.2	0.2	0.2	0.2
Oscillation (°)	0.25	0.25	0.25	0.25	0.25
Data Statistics					
Space group	P 4_3 2_1 2	P 4_3 2_1 2	P 4_3 2_1 2	P 4_3 2_1 2	P 4_3 2_1 2
Unit cell: a = b, c (Å)	77.25, 37.90	78.68, 37.04	78.57, 37.08	78.52, 37.12	78.63, 37.22
Resolution (Å)	38.62–1.15	39.34–1.00	39.28–1.05	39.26–1.05	39.31–1.05
(High shell)	(1.17–1.15)	(1.02–1.00)	(1.07–1.05)	(1.07–1.05)	(1.07–1.05)
Unique reflections	41317 (1997)	63226 (3165)	51967 (2377)	54672 (2658)	54848 (2599)
R-merge * (%)	8.0 (67.4)	3.9 (87.9)	4.4 (61.9)	4.3 (72.0)	3.8 (95.4)
I/σ(I)	22.0 (4.5)	43.7 (4.2)	41.9 (6.1)	40.1 (4.4)	43.9 (4.0)
Completeness (%)	100.0 (100.0)	100.0 (100.0)	95.3 (89.8)	100.0 (100.0)	99.8 (98.0)
Redundancy	23.7 (23.2)	24.2 (23.0)	25.6 (26.6)	24.3 (23.5)	24.5 (23.9)
B-factor ($Å^2$)	9.7	10.705	10.298	11.701	11.680
Mosaicity	0.22	0.08	0.09	0.10	0.08

Fmoc-MF and Fmoc-Y hydrogels were tested as media for protein crystallization with the model proteins lysozyme, glucose isomerase, and thaumatin, using the two-layer configuration of the counter-diffusion technique. Crystals of the three model proteins were obtained using Fmoc-MF hydrogels (Figure 1). Although the comparison of nucleation density has to be done with care when using counter-diffusion techniques, due to the evolution of the supersaturation within the length of the experiment, we observed that in the case of lysozyme, the number of crystals at low gel concentration, for instance 0.2% (*w/v*), was lower than the experiment done in agarose at 0.5% (*w/v*). This result can be explained by the well-known capability of agarose hydrogel to induce the nucleation of lysozyme [26]. It is also observed from Figure 1A that the number of crystals increased with the increasing Fmoc-MF, reaching agarose nucleation density when the concentration was 1.0% (*w/v*). Contrarily, thaumatin showed a much higher nucleation density in Fmoc-MF at any concentration than the reference experiment in agarose. As the records on the effect of agarose on the nucleation of thaumatin are not available, we cannot attribute this enhancement of nucleation to the Fmoc-MF hydrogel; it could also be an inhibition effect of agarose over the nucleation of thaumatin. In the case of glucose isomerase, there was some enhanced nucleation density in the experiments with agarose when compared to those run in Fmoc-MF, regardless of the concentration of the hydrogel. Overall, the effect could be the promotion of nucleation induced by agarose fibers or an inhibition effect of the Fmoc-MF hydrogel.

As already described for other dipeptide hydrogels [16,17], and with hydrogels in general [4], Fmoc-MF hydrogels grown with lysozyme crystals had very high quality, as shown by several crystallographic indicators (resolution limit, mosaicity, B-factor, and I/σ), and compared well with those obtained in agarose as reference (Table 2 and Table S1). The diffraction data quality from lysozyme crystals was independent of the hydrogel concentration, although some improvement was observed particularly for one of the crystals grown in 0.75% (*w/v*) being the best one of this series, as was shown not only for the highest resolution limit, 1.15 Å resolution, but also from the lower values of the

B-factor and mosaicity, which corresponded to a 20% and 40% improvement, respectively, respect to the average values.

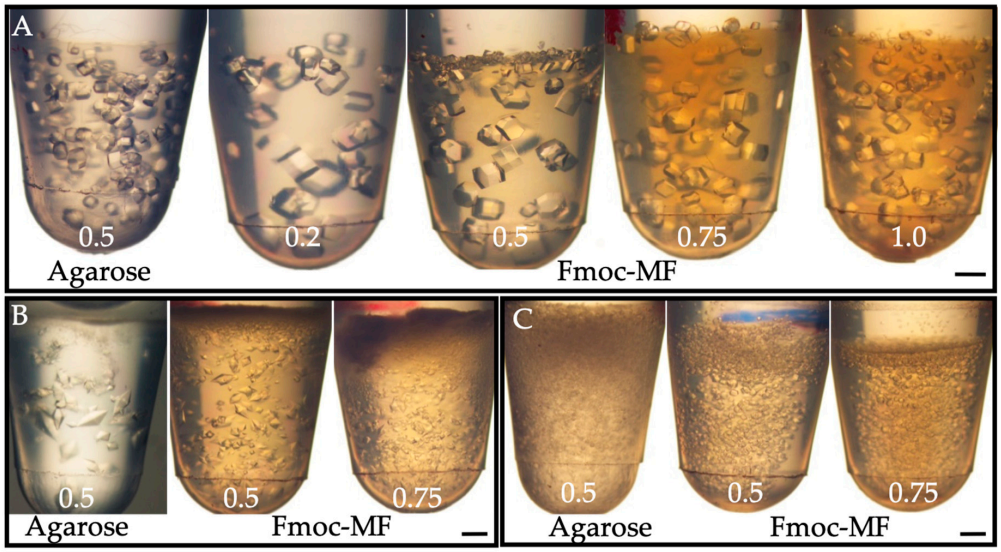

Figure 1. Lysozyme (**A**), thaumatin (**B**), and glucose isomerase (**C**) crystals obtained in agarose and Fmoc-Met-Phe-OH (Fmoc-MF) gel at different concentrations (% *w*/*v*, depicted in white number) by the 2-L counter-diffusion set-up. Scale bars correspond to 1.0 mm.

Similar results were obtained in the case of thaumatin and glucose isomerase (Table 3 and Tables S2 and S3) for which the resolution was almost the maximum attainable with the beam-line configuration, and was comparable only to those obtained also in agarose gel or under microgravity conditions [8,16,27].

In order to extend the pool of compatible hydrogel for protein crystallization, we included the already known and characterized Fmoc-Y hydrogel as crystallization media. We also studied the influence of the hydrogel concentration on the nucleation density of the lysozyme. As shown in Figure 2 and the inserts, we did not observe significant differences in the nucleation density, for the lower (0.2% *w*/*v*) and higher (1.0% *w*/*v*) hydrogel concentration, other than what was expected due to the lower diffusion rate in the higher hydrogels' concentration experiments, nor when compared with the reference experiments carried out in agarose hydrogel (Figure 1A). More relevant were the X-ray diffraction data, which were of the highest quality measured during this investigation with values of I/σ(I) over 4.0 at 1.0 Å, indicating that those crystals could diffract well at resolution higher than 1.0 Å.

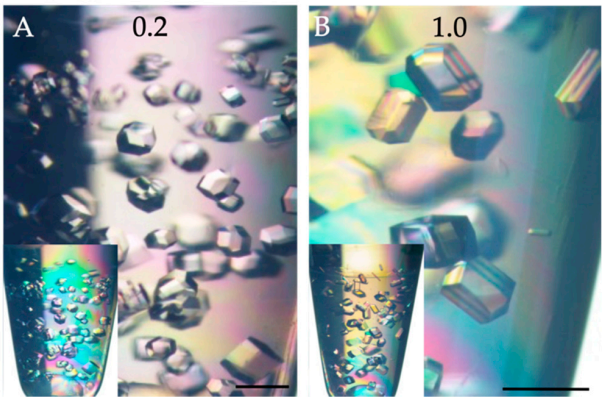

Figure 2. Lysozyme crystal grown in 0.2% *w*/*v* (**A**) and 1.0% *w*/*v* (**B**) Fmoc-Y hydrogels by the 2-L counter-diffusion technique. Inserts in the lower-left part of A and B show the whole experiment. Scale bars correspond to 1.0 mm.

4. Conclusions

We have shown in this work that two new SPS hydrogels based on methionine and tyrosine are suitable for the crystallization of proteins, namely lysozyme, thaumatin, and glucose isomerase. The obtained crystals diffracted X-rays at the maximum expected limit, demonstrating, once more, the benefits of growing crystals in media with mass transport controlled by diffusion. Contrary to the effect of other hydrogels, the range of concentration used in this work does not seem to influence the shape of crystals, which may ease the optimization process. We also show that the intrinsic composition of the hydrogel may influence the nucleation and hence the final size of the crystals. It is also important to note that since the hydrogel gets incorporated within the crystals, without disrupting the long-range ordering, the final product—that is, the hydrogel embedded in the protein periodic array—represents a distinctive composite material that may have relevant applications in biotechnology and medicine.

Supplementary Materials: The following are available online at http://www.mdpi.com/2073-4352/9/5/244/s1, Figure S1: TEM images of dried hydrogels at 0.5% *w/v*, Figure S2: (A) Fmoc-MF shear strain amplitude; (B) Fmoc-Y shear strain amplitude; (C) Fmoc-MF frequency sweeps; (D) Fmoc-Y frequency sweeps, Table S1 and S4: Summarized the data collection conditions and final statistical values of lysozyme crystals in Fmoc-MF and Fmoc-Y, respectively, compare to agarose hydrogels. Shadowed columns correspond to those already included in the main text; Table S2 and S3: Summarized the data collection conditions and final statistical values of thaumatin and glucose isomerase crystals obtained in Fmoc-MF and in agarose hydrogels. Shadowed columns correspond to those already included in the main text.

Author Contributions: Conceptualization, J.A.G. and L.A.d.-C.; hydrogel preparation, characterization and protein crystallization: G.E.-C., R.C.-M, M.-C.-M. and M.T.L.-L.; X-ray data collection and characterization: M.C.-M., A.C., J.J. and J.A.G.; writing-original draft preparation, J.A.G. and L.A.d.-C. All authors discussed the results and commented on the manuscript.

Funding: This study was supported by projects BIO2016-74875-P and FIS2017-85954-R (Ministerio de Economía, Industria y Competitividad, MINECO, and Agencia Estatal de Investigación, AEI, Spain, cofunded by Fondo Europeo de Desarrollo Regional, FEDER, European Union).

Acknowledgments: We are very grateful to the staff at XALOC of the Spanish synchrotron source (ALBA) and ID23-2 of the European Synchrotron Radiation Facility (ESRF) for support during data collection and CIC (Centro de Instrumentación Científíca). We also thank the "Unidad de Excelencia Química aplicada a Biomedicina y Medioambiente" (UGR) for support.

Conflicts of Interest: The authors declare no conflict of interest.

References

1. Henish, H.K. *Crystal Growth in Gels*; Pennsylvania State University Press: Pennsylvania, PA, USA, 1970.
2. Rizzato, S.; Moret, M.; Merlini, M.; Albinati, A.; Beghi, F. Crystal growth in gelled solution: Applications to coordination polymers. *CrystEngComm* **2016**, *18*, 2455–2462. [CrossRef]
3. Moreno, A.; Mendoza, M.E. Crystallization in Gels. In *Handbook of Crystal Growth, Second Edition*; Elsevier: Amsterdam, The Netherlands, 2015; pp. 1277–1315. [CrossRef]
4. Lorber, B.; Sauter, C.; Theobald-Dietrich, A.; Moreno, A.; Schellenberger, P.; Robert, M.-C.; Capelle, B.; Sanglier, S.; Potier, N.; Giege, R. Crystal growth of proteins, nucleic acids, and viruses in gels. *Prog. Biophys. Mol. Biol.* **2009**, *101*, 13–25. [CrossRef]
5. Gavira, J.A. Current trends in protein crystallization. *Arch. Biochem. Biophys.* **2016**, *602*, 3–11. [CrossRef]
6. García-Ruiz, J.M.; Gavira, J.A.; Otálora, F.; Guasch, A.; Coll, M. Reinforced protein crystals. *Mater. Res. Bull.* **1998**, *33*, 1593–1598. [CrossRef]
7. Sauter, C.; Balg, C.; Moreno, A.; Dhouib, K.; Théobald-Dietrich, A.; Chênevert, R.; Giegé, R.; Lorber, B. Agarose gel facilitates enzyme crystal soaking with a ligand analog. *J. Appl. Crystallogr.* **2009**, *42*, 279–283. [CrossRef]
8. Sugiyama, S.; Maruyama, M.; Sazaki, G.; Hirose, M.; Adachi, H.; Takano, K.; Murakami, S.; Inoue, T.; Mori, Y.; Matsumura, H. Growth of protein crystals in hydrogels prevents osmotic shock. *J. Am. Chem. Soc.* **2012**, *134*, 5786–5789. [CrossRef]
9. Sugiyama, S.; Shimizu, N.; Sazaki, G.; Hirose, M.; Takahashi, Y.; Maruyama, M.; Matsumura, H.; Adachi, H.; Takano, K.; Murakami, S.; et al. A Novel Approach for Protein Crystallization by a Synthetic Hydrogel with Thermoreversible Gelation Polymer. *Cryst. Growth Des.* **2013**, *13*, 1899–1904. [CrossRef]

10. Sugahara, M. A Technique for High-Throughput Protein Crystallization in Ionically Cross-Linked Polysaccharide Gel Beads for X-Ray Diffraction Experiments. *PLoS ONE* **2014**, *9*, e95017. [CrossRef] [PubMed]
11. Gavira, J.A.; Cera-Manjarres, A.; Ortiz, K.; Mendez, J.; Jimenez-Torres, J.A.; Patiño-Lopez, L.D.; Torres-Lugo, M. Use of Cross-Linked Poly(ethylene glycol)-Based Hydrogels for Protein Crystallization. *Cryst. Growth Des.* **2014**, *14*, 3239–3248. [CrossRef]
12. Buwalda, S.J.; Vermonden, T.; Hennink, W.E. Hydrogels for Therapeutic Delivery: Current Developments and Future Directions. *Biomacromolecules* **2017**, *18*, 316–330. [CrossRef]
13. Tavakoli, J.; Tang, Y. Hydrogel Based Sensors for Biomedical Applications: An Updated Review. *Polymers* **2017**, *9*. [CrossRef] [PubMed]
14. Tao, K.; Levin, A.; Adler-Abramovich, L.; Gazit, E. Fmoc-modified amino acids and short peptides: Simple bio-inspired building blocks for the fabrication of functional materials. *Chem. Soc. Rev.* **2016**, *45*, 3935–3953. [CrossRef]
15. Fleming, S.; Ulijn, R.V. Design of nanostructures based on aromatic peptide amphiphiles. *Chem. Soc. Rev.* **2014**, *43*, 8150–8177. [CrossRef] [PubMed]
16. Conejero-Muriel, M.; Gavira, J.A.; Pineda-Molina, E.; Belsom, A.; Bradley, M.; Moral, M.; Durán, J.d.D.G.-L.; Luque González, A.; Díaz-Mochón, J.J.; Contreras-Montoya, R.; et al. Influence of the chirality of short peptide supramolecular hydrogels in protein crystallogenesis. *Chem. Commun.* **2015**, *51*, 3862–3865. [CrossRef]
17. Conejero-Muriel, M.; Contreras-Montoya, R.; Díaz-Mochón, J.J.; Álvarez de Cienfuegos, L.; Gavira, J.A. Protein crystallization in short-peptide supramolecular hydrogels: A versatile strategy towards biotechnological composite materials. *CrystEngComm* **2015**, *17*, 8072–8078. [CrossRef]
18. Alvarez de Cienfuegos, L.; Gavira, J.A.; Diaz-Mochon, J.J.; Conejero-Muriel, M.T.; Contreras-Montoya, R. Pharmaceutically active protein crystals grown in-situ within a hydrogel. 2017. Available online: https://digital.csic.es/handle/10261/180548 (accessed on 9 November 2017).
19. Argudo, P.G.; Contreras-Montoya, R.; Álvarez de Cienfuegos, L.; Cuerva, J.M.; Cano, M.; Alba-Molina, D.; Martín-Romero, M.T.; Camacho, L.; Giner-Casares, J.J. Unravelling the 2D self-assembly of Fmoc-dipeptides at fluid interfaces. *Soft. Matter.* **2018**, *14*, 9343–9350. [CrossRef]
20. Contreras-Montoya, R.; Bonhome-Espinosa, A.B.; Orte, A.; Miguel, D.; Delgado-López, J.M.; Duran, J.D.G.; Cuerva, J.M.; Lopez-Lopez, M.T.; Álvarez de Cienfuegos, L. Iron nanoparticles-based supramolecular hydrogels to originate anisotropic hybrid materials with enhanced mechanical strength. *Mater. Chem. Front.* **2018**, *2*, 686–699. [CrossRef]
21. Mahler, A.; Reches, M.; Rechter, M.; Cohen, S.; Gazit, E. Rigid, Self-Assembled Hydrogel Composed of a Modified Aromatic Dipeptide. *Adv. Mater.* **2006**, *18*, 1365–1370. [CrossRef]
22. Juanhuix, J.; Gil-Ortiz, F.; Cuní, G.; Colldelram, C.; Nicolás, J.; Lidón, J.; Boter, E.; Ruget, C.; Ferrer, S.; Benach, J. Developments in optics and performance at BL13-XALOC, the macromolecular crystallography beamline at the Alba Synchrotron. *J. Synchrotron Radiat.* **2014**, *21*, 679–689. [CrossRef] [PubMed]
23. Flot, D.; Mairs, T.; Giraud, T.; Guijarro, M.; Lesourd, M.; Rey, V.; van Brussel, D.; Morawe, C.; Borel, C.; Hignette, O.; et al. The ID23-2 structural biology microfocus beamline at the ESRF. *J. Synchrotron Radiat.* **2009**, *17*, 107–118. [CrossRef] [PubMed]
24. Yang, Z.; Gu, H.; Fu, D.; Gao, P.; Lam, J.K.; Xu, B. Enzymatic Formation of Supramolecular Hydrogels. *Adv. Mater.* **2004**, *16*, 1440–1444. [CrossRef]
25. Yang, Z.; Xu, B. A simple visual assay based on small molecule hydrogels for detecting inhibitors of enzymes. *Chem. Commun.* **2004**, *21*, 2424–2425. [CrossRef] [PubMed]
26. Vidal, O.; Robert, M.C.; Boué, F. Gel growth of lysozyme crystals studied by small angle neutron scattering: Case of agarose gel, a nucleation promotor. *J. Cryst. Growth* **1998**, *192*, 257–270. [CrossRef]
27. Sauter, C.; Lorber, B.; Giege, R. Towards atomic resolution with crystals grown in gel: The case of thaumatin seen at room temperature. *Proteins* **2002**, *48*, 146–150. [CrossRef] [PubMed]

© 2019 by the authors. Licensee MDPI, Basel, Switzerland. This article is an open access article distributed under the terms and conditions of the Creative Commons Attribution (CC BY) license (http://creativecommons.org/licenses/by/4.0/).